Engineering Analysis with Boundary Elements 33 (2009) 547–554

Contents lists available at ScienceDirect

Engineering Analysis with Boundary Elements

journal homepage: www.elsevier.com/locate/enganabound

Improved element-free Galerkin method for two-dimensional potential problems

Zan Zhang [a], Peng Zhao [b], K.M. Liew [a,*]

[a] Department of Building and Construction, City University of Hong Kong, Tat Chee Avenue, Kowloon, Hong Kong
[b] School of Computer Science and Technology, Shandong University, Jinan 250101, China

ARTICLE INFO

Article history:
Received 9 November 2007
Accepted 10 August 2008
Available online 25 September 2008

Keywords:
Weighted orthogonal function
Improved moving least-squares (IMLS) approximation
Meshless method
Element-free Galerkin (EFG) method
Improved element-free Galerkin (IEFG) method
Potential problem

ABSTRACT

Potential difficulties arise in connection with various physical and engineering problems in which the functions satisfy a given partial differential equation and particular boundary conditions. These problems are independent of time and involve only space coordinates, as in Poisson's equation or the Laplace equation with Dirichlet, Neuman, or mixed conditions. When the problems are too complex, they usually cannot be solved with analytical solutions. The element-free Galerkin (EFG) method is a meshless method for solving partial differential equations on which the trial and test functions employed in the discretization process result from moving least-squares (MLS) interpolants. In this paper, by using the weighted orthogonal basis function to construct the MLS interpolants, we derive the formulae of an improved EFG (IEFG) method for two-dimensional potential problems. There are fewer coefficients in the improved MLS (IMLS) approximation than in the MLS approximation, and in the IEFG method fewer nodes are selected in the entire domain than in the conventional EFG method. Hence, the IEFG method should result in a higher computing speed.

1. Introduction

Partial differential equations arise in connection with various physical and geometrical problems in which the functions involved depend on two or more independent variables, usually on time t and on one or several space variables [1].

A potential problem is one of the most important partial differential equations in engineering mathematics, because it occurs in connection with gravitational fields, electrostatics fields, steady-state heat conduction, incompressible fluid flow, and other areas [1]. Mathematically, the problem is a function that satisfies a given partial differential equation and particular boundary conditions (boundary-value problems). Physically speaking, the problem is independent of time and involves only space coordinates, just as initial-value problems are associated with hyperbolic partial differential equations of the elliptic type. In contrast to initial-value problems, boundary-value problems are considerably more difficult to solve. This is due to the physical requirement that solutions must attain in the large, unlike the case of initial-value problems, in which solutions in the small, say over a short interval of time, may still be of physical interest [2]. Well-known potential problems include the Laplace or Poisson's equation in a given domain with a condition on the boundary.

When the figures or the boundary conditions of the discussed object are too complex, they usually cannot be solved with analytical solutions. In this paper, two-dimensional (2D) potential problems are investigated using a meshless method: the improved element-free Galerkin (IEFG) method.

Meshless methods in computational mechanics have attracted much attention in recent decades. They can also be used to solve many engineering problems that do not lend themselves to solution using such traditional methods as the finite element method (FEM) or the boundary element method (BEM), especially extremely large deformation, dynamic fracturing, and explosion problems [3–5]. The main objective of meshless methods is to get rid of, or at least to alleviate, the difficulty of meshing and remeshing the entire structure by simply adding or deleting nodes.

The main difference between meshless methods and conventional numerical methods is the way in which the shape function is formulated. However, once the shape function has been obtained, the meshless method, the FEM, and the BEM use the same procedure to form the equations to obtain the solution to a problem [5].

Many meshless methods have been developed, including the diffuse element method (DEM) [6], the element-free Galerkin (EFG) method [7], the Hp clouds method [8], the finite point

* Corresponding author.
E-mail address: kmliew@cityu.edu.hk (K.M. Liew).

0955-7997/$ - see front matter © 2008 Elsevier Ltd. All rights reserved.
doi:10.1016/j.enganabound.2008.08.004

method (FPM) [9], the meshless local Petrov–Galerkin (MLPG) method [10], the multi-scale reproducing kernel particle (MRKP) method [11], the wavelet particle method (WPM) [12], the radial basis functions (RBF) method [13], the meshless FEM (MFEM) [14], the element-free kp-Ritz method [15], the complex variable meshless method [16], and the meshless method with boundary integral equation [17–20]. Of these, the EFG method is the most widely applied.

The EFG method was developed by Belytschko et al. [7] based on the DEM originated by Nayroles et al. [6]. One of the major features of EFG methods is that the moving least-square (MLS) approximation is employed for the construction of the shape function [21]. To use MLS interpolants, the approximated field function is continuous and smooth in the entire problem domain, and it is capable of producing an approximation with the desired order of consistency [22].

The MLS approximation was developed from the conventional least-squares method, and in practical numerical processes it essentially involves the application of the conventional method to every selected point. A disadvantage of the conventional least-squares method is that the final algebra equations system is sometimes ill conditioned. Hence, in the MLS approximation, the ill-conditioned algebra equations system must be solved. However, it is difficult to determine which algebra equations system is ill conditioned, as there are no methods in mathematical theory for judging whether such a system is ill conditioned before the equation is solved. Thus, we sometimes cannot obtain a good solution or even a correct numerical solution.

A new method of obtaining the approximation function—the improved MLS (IMLS) approximation—has been developed [19,20]. In the IMLS, the orthogonal function system with a weight function is used as the basis function. The algebra equations system in the IMLS approximation is not ill conditioned, and it can be solved without having to derive the inverse matrix. There are also fewer coefficients in the IMLS approximation than in the MLS approximation, and hence the computing speed and the efficiency with which a solution is found are greater.

Based on the IMLS approximation and the EFG method, an improved EFG (IEFG) method is created [23,24]. This method in then used to solve 2D potential problems. Because there are fewer coefficients in the IMLS than there are in the MLS approximation, in the IEFG method that is formed with the IMLS approximation, fewer nodes are selected in the entire domain than are selected in the conventional EFG method. Hence, the IEFG method should result in a higher computing speed. Furthermore, the IEFG method has greater computational precision than does the EFG method when the same nodes are selected in the domain.

2. MLS approximation

2.1. MLS interpolants function

In the EFG method, MLS approximation is employed for the construction of the shape function.

Let $u(\boldsymbol{x})$ be the function of the field variable defined in the domain Ω. The approximation of $u(\boldsymbol{x})$ at point $\boldsymbol{x}$ is denoted $u^h(\boldsymbol{x})$, and the trial function is

$$u^h(\boldsymbol{x}) = \sum_{i=1}^{m} p_i(\boldsymbol{x}) a_i(\boldsymbol{x}) = \boldsymbol{p}^{\mathrm{T}}(\boldsymbol{x})\boldsymbol{a}(\boldsymbol{x}), \tag{1}$$

where $\boldsymbol{p}(\boldsymbol{x})$ is a vector of basis functions that consists most often of monomials of the lowest order to ensure minimum completeness, m is the number of terms of the monomials, and $\boldsymbol{a}(\boldsymbol{x})$ is a vector of coefficients given by

$$\boldsymbol{a}^{\mathrm{T}}(x) = (a_0(x), a_1(x), \ldots, a_m(x)), \tag{2}$$

which are functions of $\boldsymbol{x}$. In the 2D, the following basis can be chosen:

$$\boldsymbol{p}^{\mathrm{T}}(\boldsymbol{x}) = (1, x, y) \quad (m = 3, \text{ linear basis}) \tag{3}$$

or

$$\boldsymbol{p}^{\mathrm{T}}(\boldsymbol{x}) = (1, x, y, xy, x^2, y^2) \quad (m = 6, \text{ quadratic basis}). \tag{4}$$

The local approximation at $\boldsymbol{x}$, as described by Lancaster and Salkauskas [21], is

$$u^h(\boldsymbol{x}, \bar{\boldsymbol{x}}) = \sum_{i=1}^{m} p_i(\bar{\boldsymbol{x}}) a_i(\boldsymbol{x}) = \boldsymbol{p}^{\mathrm{T}}(\bar{\boldsymbol{x}})\boldsymbol{a}(\boldsymbol{x}), \tag{5}$$

where $\bar{\boldsymbol{x}}$ is the point in the local approximation of $\boldsymbol{x}$.

To obtain the local approximation of the function $u(\boldsymbol{x})$, the difference between the local approximation $u^h(\boldsymbol{x})$ and the function $u(\boldsymbol{x})$ must be minimized by a weighted least-squares method.

Define a function

$$\begin{aligned} J &= \sum_{I=1}^{n} w(\boldsymbol{x} - \boldsymbol{x}_I)[u^h(\boldsymbol{x}, \boldsymbol{x}_I) - u(\boldsymbol{x}_I)]^2 \\ &= \sum_{I=1}^{n} w(\boldsymbol{x} - \boldsymbol{x}_I)\left[\sum_{i=1}^{m} p_i(\boldsymbol{x}_I) \cdot a_i(\boldsymbol{x}) - u(\boldsymbol{x}_I)\right]^2, \end{aligned} \tag{6}$$

where $w(\boldsymbol{x}-\boldsymbol{x}_I)$ is a weight function with a domain of influence, and $\boldsymbol{x}_I$ ($I = 1, 2, \ldots, n$) are the nodes with domains of influence that cover the point $\boldsymbol{x}$.

Eq. (6) can be written as

$$J = (\boldsymbol{P}\boldsymbol{a} - \boldsymbol{u})^{\mathrm{T}} \boldsymbol{W}(\boldsymbol{x})(\boldsymbol{P}\boldsymbol{a} - \boldsymbol{u}), \tag{7}$$

where

$$\boldsymbol{u}^{\mathrm{T}} = (u_1, u_2, \ldots, u_n), \tag{8}$$

$$\boldsymbol{P} = \begin{bmatrix} p_1(x_1) & p_2(x_1) & \ldots & p_m(x_1) \\ p_1(x_2) & p_2(x_2) & \ldots & p_m(x_2) \\ \vdots & \vdots & \ddots & \vdots \\ p_1(x_n) & p_2(x_n) & \ldots & p_m(x_n) \end{bmatrix}, \tag{9}$$

$$\boldsymbol{W}(\boldsymbol{x}) = \begin{bmatrix} w(\boldsymbol{x} - \boldsymbol{x}_1) & 0 & \ldots & 0 \\ 0 & w(\boldsymbol{x} - \boldsymbol{x}_2) & \ldots & 0 \\ \vdots & \vdots & \ddots & \vdots \\ 0 & 0 & \ldots & w(\boldsymbol{x} - \boldsymbol{x}_n) \end{bmatrix}. \tag{10}$$

The minimization condition requires

$$\frac{\partial J}{\partial \boldsymbol{a}} = 0, \tag{11}$$

which results in the equation system

$$\boldsymbol{A}(\boldsymbol{x})\boldsymbol{a}(\boldsymbol{x}) = \boldsymbol{B}(\boldsymbol{x})\boldsymbol{u}, \tag{12}$$

where matrices $\boldsymbol{A}(\boldsymbol{x})$ and $\boldsymbol{B}(\boldsymbol{x})$ are

$$\boldsymbol{A}(\boldsymbol{x}) = \boldsymbol{p}^{\mathrm{T}} \boldsymbol{W}(\boldsymbol{x})\boldsymbol{p}, \tag{13}$$

$$\boldsymbol{B}(\boldsymbol{x}) = \boldsymbol{p}^{\mathrm{T}} \boldsymbol{W}(\boldsymbol{x}). \tag{14}$$

$\boldsymbol{u}$ is the vector that collects the nodal parameters of the field variables for all of the nodes in the support domain.

From Eq. (12), we can obtain

$$\boldsymbol{a}(\boldsymbol{x}) = \boldsymbol{A}^{-1}(\boldsymbol{x})\boldsymbol{B}(\boldsymbol{x})\boldsymbol{u}. \tag{15}$$

The expression of the local approximation $u^h(\boldsymbol{x})$ is thus

$$u^h(\boldsymbol{x}) = \boldsymbol{\Phi}(\boldsymbol{x})\boldsymbol{u} = \sum_{I=1}^{h} \Phi_I(\boldsymbol{x})u_I, \tag{16}$$

where $\boldsymbol{\Phi}(\boldsymbol{x})$ is the MLS shape function and

$$\boldsymbol{\Phi}(\boldsymbol{x}) = (\Phi_1(\boldsymbol{x}), \Phi_2(\boldsymbol{x}), \ldots, \Phi_n(\boldsymbol{x})) = \boldsymbol{p}^{\mathrm{T}}(\boldsymbol{x})\boldsymbol{A}^{-1}(\boldsymbol{x})\boldsymbol{B}(\boldsymbol{x}). \tag{17}$$

2.2. The orthogonal basis functions

In an MLS approximation, Eq. (12) is sometimes ill conditioned, even in the presence of a singular phenomenon. Moreover, it is difficult to obtain the correct numerical solution. Using the weighted orthogonal basis functions, the IMLS approximation was presented [19,20].

For $\forall f(\boldsymbol{x}), g(\boldsymbol{x}) \in span(\boldsymbol{p})$, define

$$(f,g) = \sum_{I=1}^{n} w(\boldsymbol{x} - \boldsymbol{x}_I) f(\boldsymbol{x}_I) g(\boldsymbol{x}_I), \tag{18}$$

and then (f,g) is an inner product, and $span(\boldsymbol{p})$ is a Hilbert space.

In the Hilbert space $span(\boldsymbol{p})$, for the set of points $\{\boldsymbol{x}_i\}$ and the weight functions $\{w_i\}$, if the functions $p_1(\boldsymbol{x})$, $p_2(\boldsymbol{x})$,…, $p_m(\boldsymbol{x})$ satisfy the conditions

$$(p_k, p_j) = \sum_{i=1}^{n} w_i p_k(\boldsymbol{x}_i) p_j(\boldsymbol{x}_i) = \begin{cases} 0, & k \neq j \\ A_k, & k = j \end{cases} \quad (k,j = 1,2,\ldots,m), \tag{19}$$

then the function set $p_1(\boldsymbol{x})$, $p_2(\boldsymbol{x})$,…, $p_m(\boldsymbol{x})$ is called a weighted orthogonal function set with a weight function $\{w_i\}$ about points $\{\boldsymbol{x}_i\}$. If $p_1(\boldsymbol{x})$, $p_2(\boldsymbol{x})$,…, $p_m(\boldsymbol{x})$ are polynomials, then the function set $p_1(\boldsymbol{x})$, $p_2(\boldsymbol{x})$,…, $p_m(\boldsymbol{x})$ is called a weighted orthogonal polynomials set with the weight functions $\{w_i\}$ about points $\{\boldsymbol{x}_i\}$.

From Eq. (18), Eq. (12) can be written as

$$\begin{bmatrix} (p_1,p_1) & (p_1,p_2) & \ldots & (p_1,p_m) \\ (p_2,p_1) & (p_2,p_2) & \ldots & (p_2,p_m) \\ \vdots & \vdots & \ddots & \vdots \\ (p_m,p_1) & (p_m,p_2) & \ldots & (p_m,p_m) \end{bmatrix} \begin{bmatrix} a_1(\boldsymbol{x}) \\ a_2(\boldsymbol{x}) \\ \vdots \\ a_m(\boldsymbol{x}) \end{bmatrix} = \begin{bmatrix} (p_1,u_I) \\ (p_2,u_I) \\ \vdots \\ (p_m,u_I) \end{bmatrix}. \tag{20}$$

If the basis function set $p_i(\boldsymbol{x}) \in span(\boldsymbol{p})$, $I = 1, 2,\ldots, m$, is a weighted orthogonal function set about points $\{\boldsymbol{x}_i\}$, i.e., if

$$(p_i, p_j) = 0, \quad (i \neq j), \tag{21}$$

then Eq. (20) becomes

$$\begin{bmatrix} (p_1,p_1) & 0 & \ldots & 0 \\ 0 & (p_2,p_2) & \ldots & 0 \\ \vdots & \vdots & \ddots & \vdots \\ 0 & 0 & \ldots & (p_m,p_m) \end{bmatrix} \begin{bmatrix} a_1(\boldsymbol{x}) \\ a_2(\boldsymbol{x}) \\ \vdots \\ a_m(\boldsymbol{x}) \end{bmatrix} = \begin{bmatrix} (p_1,u_I) \\ (p_2,u_I) \\ \vdots \\ (p_m,u_I) \end{bmatrix}. \tag{22}$$

We can then directly obtain the coefficients $a_i(\boldsymbol{x})$ as follows:

$$a_i(\boldsymbol{x}) = \frac{(p_i,u_I)}{(p_i,p_i)} \quad (i = 1,2,\ldots,m), \tag{23}$$

i.e.,

$$\boldsymbol{a}(\boldsymbol{x}) = \bar{\boldsymbol{A}}(\boldsymbol{x})\boldsymbol{B}(\boldsymbol{x})\boldsymbol{u}, \tag{24}$$

where

$$\bar{\boldsymbol{A}}(\boldsymbol{x}) = \begin{bmatrix} \frac{1}{(p_1,p_1)} & 0 & \ldots & 0 \\ 0 & \frac{1}{(p_2,p_2)} & \ldots & 0 \\ \vdots & \vdots & \ddots & \vdots \\ 0 & 0 & \ldots & \frac{1}{(p_m,p_m)} \end{bmatrix}. \tag{25}$$

From Eqs. (23) and (5), the expression of the approximation function $u^h(\boldsymbol{x})$ is

$$u^h(\boldsymbol{x}) = \bar{\boldsymbol{\Phi}}(\boldsymbol{x})\boldsymbol{u} = \sum_{I=1}^{n} \overline{\Phi}_I(\boldsymbol{x})u_I, \tag{26}$$

where $\bar{\boldsymbol{\Phi}}(\boldsymbol{x})$ is the shape function and

$$\bar{\boldsymbol{\Phi}}(\boldsymbol{x}) = (\overline{\Phi}_1(\boldsymbol{x}), \overline{\Phi}_2(\boldsymbol{x}), \ldots, \overline{\Phi}_n(\boldsymbol{x})) = \boldsymbol{p}^{\mathrm{T}}(\boldsymbol{x})\bar{\boldsymbol{A}}(\boldsymbol{x})\boldsymbol{B}(\boldsymbol{x}). \tag{27}$$

This is an IMLS approximation in which the coefficients $a_i(\boldsymbol{x})$ are obtained simply and directly. It is therefore impossible to form an ill-conditioned or singular equations system, and we can thus obtain the correct solution.

From Eq. (27), we have

$$\overline{\Phi}_I(\boldsymbol{x}) = \sum_{j=1}^{m} p_j(\boldsymbol{x})[\bar{\boldsymbol{A}}(\boldsymbol{x})\boldsymbol{B}(\boldsymbol{x})]_{jI}, \tag{28}$$

which represents the shape function of the IMLS approximation corresponding node I. Then, the partial derivatives of $\overline{\Phi}_I(\boldsymbol{x})$ can be obtained as

$$\overline{\Phi}_{I,i}(\boldsymbol{x}) = \sum_{j=1}^{m} [p_{j,i}(\bar{\boldsymbol{A}}\boldsymbol{B})_{jI} + p_j(\bar{\boldsymbol{A}}_i\boldsymbol{B} + \bar{\boldsymbol{A}}\boldsymbol{B}_i)_{jI}]. \tag{29}$$

The weighted orthogonal basis function set $\boldsymbol{p} = (p_i)$ can be formed with the Schmidt method,

$$p_1 = 1,$$
$$p_i = r^{i-1} - \sum_{k=1}^{i-1} \frac{(r^{i-1}, p_k)}{(p_k, p_k)} p_k, \quad i = 2,3,\ldots \tag{30}$$

or can be expressed as

$$p_1 = 1,$$
$$p_2 = r - a_2,$$
$$p_i = (r - a_i)p_{i-1} - b_i p_{i-2}, \quad i = 3,4,\ldots, \tag{31}$$

where

$$a_i = \frac{(rp_{i-1}, p_{i-1})}{(p_{i-1}, p_{i-1})}, \tag{32}$$

$$b_i = \frac{(p_{i-1}, p_{i-1})}{(p_{i-2}, p_{i-2})}, \tag{33}$$

and $r = \sqrt{x_1^2 + x_2^2}$ or $r = x_1 + x_2$ for 2D problems.

In addition, using the Schmidt method, the weighted orthogonal basis function set $\boldsymbol{p} = (p_i)$ can be formed from the monomial basis function. For example, for the monomial basis function

$$\bar{\boldsymbol{p}} = (\bar{p}_i) = (1, x_1, x_2, x_1^2, x_1, x_2, x_2^2, \ldots), \tag{34}$$

the weighted orthogonal basis function set can be formed as

$$p_i = \bar{p}_i - \sum_{k=1}^{i-1} \frac{(\bar{p}_i, p_k)}{(p_k, p_k)} p_k, \quad i = 1,2,3,\ldots. \tag{35}$$

When the weighted orthogonal basis functions (30) and (31) are used, there are fewer coefficients in the trial function. In an IMLS approximation, fewer nodes are needed in a domain of influence than in an MLS approximation. Thus, with the meshless

method that is formed with an IMLS approximation, fewer nodes are selected than with the conventional meshless methods in the whole domain.

2.3. Weight function

The weight function used in (6)–(17) plays an important role in the EFG method. The weight function should be non-zero over only a small neighborhood of x_I to generate a set of sparse discrete equations.

Define $d_I = \|x-x_I\|$ and $r = d_I/d_{mI}$, where d_{mI} is the size of the domain of influence of the Ith node. Then, the weight function can be written as a function of the normalized radius r. In this paper, we use the cubic spline weight function

$$w(x-x_I) \equiv w(r) = \begin{cases} \frac{2}{3} - 4r^2 + 4r^3, & r \leqslant \frac{1}{2}, \\ \frac{4}{3} - 4r + 4r^2 - \frac{4}{3}r^3, & \frac{1}{2} < r \leqslant 1, \\ 0, & r > 1. \end{cases} \tag{36}$$

The size of the domain of influence at a node, d_{mI}, is computed by

$$d_{mI} = d_{\max} c_I, \tag{37}$$

where $d_{\max}$ is a scaling parameter. The distance c_I is determined by searching for enough neighbor nodes for $\boldsymbol{A}$ to be regular, i.e., invertible. Due to (29), we must compute the spatial derivative of the weight function as

$$\frac{\mathrm{d}w_I}{\mathrm{d}x} = \frac{\mathrm{d}w_I}{\mathrm{d}r}\frac{\mathrm{d}r}{\mathrm{d}x} = \begin{cases} (-8r + 12r^2 \mathrm{sign}(x-x_I), & \text{for } r \leqslant \frac{1}{2}, \\ (-4 + 8r - 4r^2)\mathrm{sign}(x-x_I), & \text{for } \frac{1}{2} \leqslant r \leqslant 1, \\ 0, & \text{for } r > 1. \end{cases} \tag{38}$$

3. IEFG method for 2D potential problems

3.1. 2D potential formulations

Consider a Poisson's equation for a problem governing the potential u in a 2D domain Ω bounded by contour Γ (see Fig. 1):

$$\nabla \cdot \boldsymbol{u}(\boldsymbol{x}) + \boldsymbol{f}(\boldsymbol{x}) = 0, \quad \text{in } \Omega, \tag{39}$$

where $\boldsymbol{f}(\boldsymbol{x})$ is a given source function of x and y. In the general case, the boundary Γ can have mixed boundary conditions. On one part of the boundary Γ_u, the potential u is prescribed, and, on the remaining part, Γ_σ, the secondary variables, flux ($q = \mathrm{d}u/\mathrm{d}n$), are prescribed, i.e.,

$$\boldsymbol{u}(\boldsymbol{x}) = \bar{\boldsymbol{u}}(\boldsymbol{x}), \quad \boldsymbol{x} \in \Gamma_{\boldsymbol{u}}, \tag{40}$$

$$\boldsymbol{q}(\boldsymbol{x}) \equiv \frac{\partial u(\boldsymbol{x})}{\partial n} = \bar{q}(\boldsymbol{x}), \quad x \in \Gamma_q, \tag{41}$$

where the boundary $\Gamma = \partial\Omega = \Gamma_u + \Gamma_q$, and $\boldsymbol{n}$ is the unit outward normal to the boundary. For example, in a steady-state heat transfer problem, which is a topical Poisson's problem, u is the temperature, q is the heat flux function, and $\boldsymbol{f}(\boldsymbol{x})$ is internal heat generation.

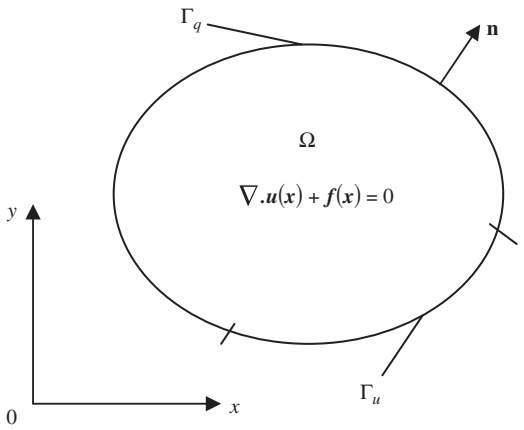

Fig. 1. Two-dimensional potential problem.

3.2. IEFG with penalty method

The use of the MLS approximation produces shape functions that do not possess the Kronecker delta function property, i.e., $\phi_I(x_J) \neq \delta_{IJ}$, and therefore $u^h(x_J) \neq u_J$. This implies that essential boundary conditions cannot be imposed in the same way that they can in conventional FEM [22].

In this paper, we enforce essential boundary conditions using penalty factors. The use of the penalty method produces equation systems of the same dimensions that FEM produces for the same number of nodes, and the modified stiffness matrix is still positively defined [22]; moreover, the symmetry and the bandedness of the system matrix are preserved. These advantages make the penalty method much more efficient than the Lagrange multipliers method.

In the EFG method, the essential boundary conditions that need to be enforced have the form

$$\sum_I^n \phi_I(\boldsymbol{x})\boldsymbol{u}_I = \bar{\boldsymbol{u}}(\boldsymbol{x}) \quad \text{on } \Gamma_u, \tag{42}$$

where $\bar{u}(\boldsymbol{x})$ is the prescribed displacement on the essential boundary.

Now, consider the problem stated in Eqs. (36)–(38). We introduce a penalty factor to penalize the difference between the displacement of the MLS approximation and the prescribed displacement on the essential boundary. The constrained Galerkin weak form using the penalty method can then be posed as

$$\int_\Omega \delta(\nabla u)^{\mathrm{T}} \nabla u \,\mathrm{d}\Omega - \int_\Omega \delta u^{\mathrm{T}} f \,\mathrm{d}\Omega - \int_{\Gamma_u} \bar{q}\delta u \,\mathrm{d}\Gamma + \frac{\alpha}{2}\delta \int_{\Gamma_u} (u-\bar{u})^{\mathrm{T}}(u-\bar{u}) \,\mathrm{d}\Gamma = 0, \tag{43}$$

where $\alpha = (\alpha_1, \alpha_2, \ldots, \alpha_k)$ is a diagonal matrix of the penalty factor, where $k = 2$ for 2D and $k = 3$ for 3D cases. The penalty factors α_i ($i = 1, \ldots, k$) can be a function of the coordinates, and they can be different from one another, although in practice we often assign them the identical constant of a large positive number, which can be chosen by following the method [22]:

$$\boldsymbol{\alpha} = 1.0 \times 10^{4-13} \times \max(\text{diagonal element in the stiffness matrix}). \tag{44}$$

Substituting Eq. (26) (which is the approximation function of the IMLS) and Eq. (44) into Eq. (43), we arrive at the final system equation of

$$[\boldsymbol{K} + \boldsymbol{K}^{\alpha}]\boldsymbol{u} = \boldsymbol{F} + \boldsymbol{F}^{\alpha}, \tag{45}$$

where

$$\boldsymbol{K}_{IJ} = \int_\Omega (\overline{\Phi}_{I,x}\overline{\Phi}_{J,x} + \overline{\Phi}_{I,y}\overline{\Phi}_{J,y}) \,\mathrm{d}\Omega, \tag{46}$$

$$\boldsymbol{F}_I = \int_{\Gamma_\sigma} \overline{\Phi}_I^{\mathrm{T}} \bar{\boldsymbol{q}} \,\mathrm{d}\Gamma + \int_\Omega \overline{\Phi}_I^{\mathrm{T}} \boldsymbol{f} \,\mathrm{d}\Omega. \tag{47}$$

The additional matrix $\boldsymbol{K}^{\alpha}$ is the global penalty matrix assembled using the nodal matrix defined by

$$K_{IJ}^{\alpha} = \int_{\Gamma_u} \bar{\boldsymbol{\Phi}}_I^{\mathrm{T}} \boldsymbol{\alpha} \bar{\boldsymbol{\Phi}}_J \, \mathrm{d}\Gamma. \tag{48}$$

The vector $\boldsymbol{F}^{\alpha}$ is caused by the essential boundary condition, and its nodal vector has the form

$$F_I^{\alpha} = \int_{\Gamma_u} \bar{\boldsymbol{\Phi}}_I^{J} \boldsymbol{\alpha} \bar{\boldsymbol{u}} \, \mathrm{d}\Gamma. \tag{49}$$

4. Convergence study

The convergence study of the proposed method on 2D potential problems is carried out by analyzing the final potential function values under different discretization schemes and different scaling factors $d_{\max}$ for the nodes of the study field. For example, we apply this method on the 2D Poisson's equation with Dirichlet boundary conditions on the rectangular domain. The government equation and the boundary conditions are

$$\frac{\partial^2 u}{\partial x^2} + \frac{\partial^2 u}{\partial y^2} - 4 = 0, \quad x \in [0,8], \ \ y \in [-3,3], \tag{50}$$

$$u(0,y) = y^2, \quad -3 < x < 3, \tag{51}$$

$$u(8,y) = 64 + y^2, \quad -3 < y < 3, \tag{52}$$

$$T(x,3) = x^2 + 9, \quad 0 < x < 8, \tag{53}$$

and

$$T(x,-3) = x^2 + 9, \quad 0 < x < 8. \tag{54}$$

The analytical solution of this problem is

$$u(x,y) = x^2 + y^2. \tag{55}$$

Figs. 2–5 show the variations along the y direction, where $x = 3$, using both the EFG and IEFG methods.

One the one hand, using a certain number of nodes, we resize the values of $d_{\max}$. From Figs. 2 and 3, we can see that for both the EFG and IEFG methods when $d_{\max}$ ranges from 1.5 to 2.1, we can get the same results. Although the difference among the values obtained from different $d_{\max}$ is very small and the results gradually approach the analytical solution with the same convergence speed, the IEFG method has a faster computer time than using the EFG method.

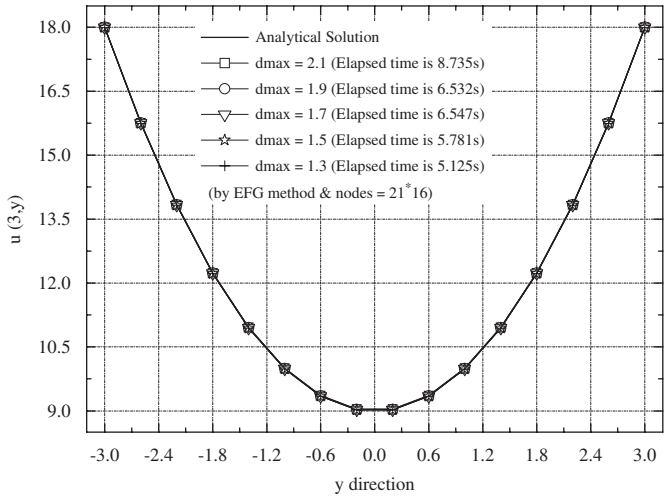

Fig. 2. Values given by EFG method along y-axis under different $d_{\max}$ with a certain number of nodes.

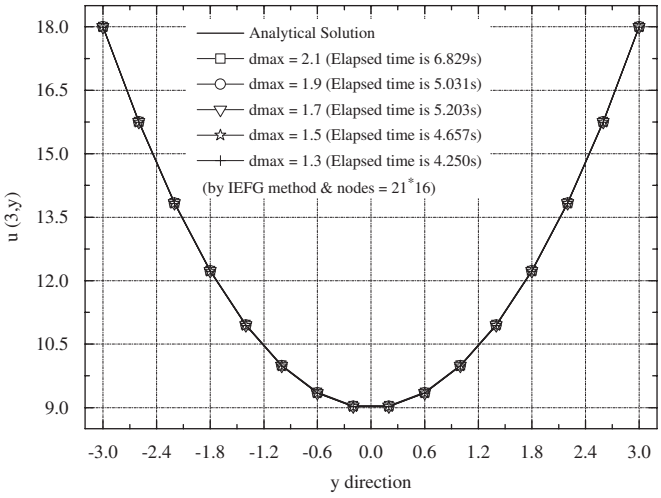

Fig. 3. Results computed by IEFG method under different $d_{\max}$ with a stated node.

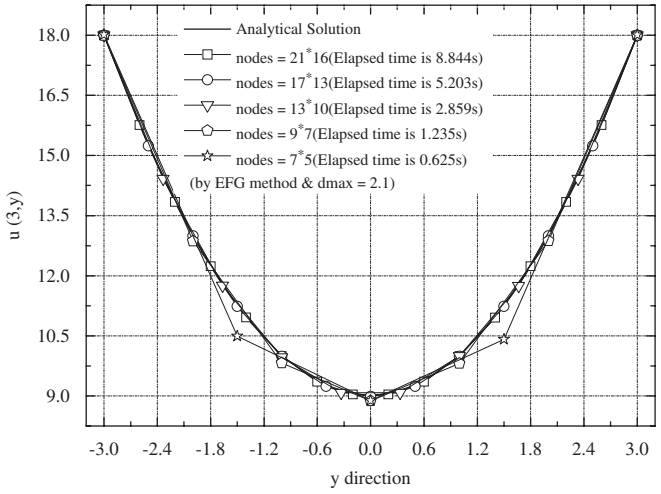

Fig. 4. Use EFG method with different nodes at $d_{\max} = 2.1$.

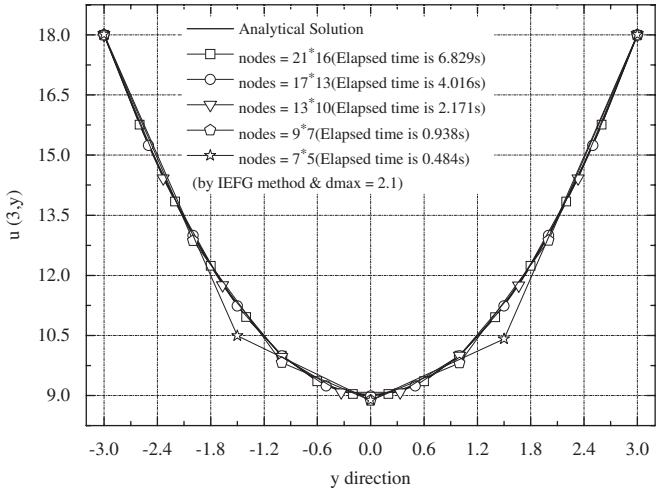

Fig. 5. IEFG method with different nodes at $d_{\max} = 2.1$.

On the other hand, Figs. 4 and 5 show that, with different nodes under certain $d_{\max}$, the solution converges when the number of nodes increase, so higher completeness orders of the

basis function can achieve better convergence characteristics than lower orders. Similar to the method state above, the EFG and IEFG methods can give the same results and have the same convergence speed, but different computer times.

5. Example problems

Three example problems are presented to demonstrate the applicability of the IEFG with the penalty method for 2D potential problems. The results that are obtained for these examples are compared with the EFG method and existing analytical solutions that have been published in the literature.

A regular or irregular arrangement of nodes and the background mesh of cells are used for numerical integrations to calculate the system equation. In each integration cell, a 4×4 Gauss quadrature scheme is used to evaluate the stiffness matrix. The weighted orthogonal basis and cubic spline weight function are used in the IMLS approximation.

5.1. Poisson's equation with Dirichlet problems on a torus

The first example is a 2D Poisson's equation with Dirichlet boundary conditions on the torus, as shown in Fig. 6. The Poisson's equation is

$$\frac{\partial^2 u}{\partial x^2}+\frac{\partial^2 u}{\partial y^2}-4=0,\quad a<r<b,\ \ 0<\theta<2\pi. \tag{56}$$

The boundary conditions are

$$u(a,\theta)=0, \tag{57}$$

$$u(b,\theta)=0. \tag{58}$$

The analytical solution of this problem is

$$u(r,\theta)=(r^2-a^2)-(b^2-d^2)\left(\frac{\log r-\log a}{\log a-\log b}\right). \tag{59}$$

There, we suppose $a=1$ and $b=2$. The analytical solution and the numerical solution using both the IEFG and EFG method along

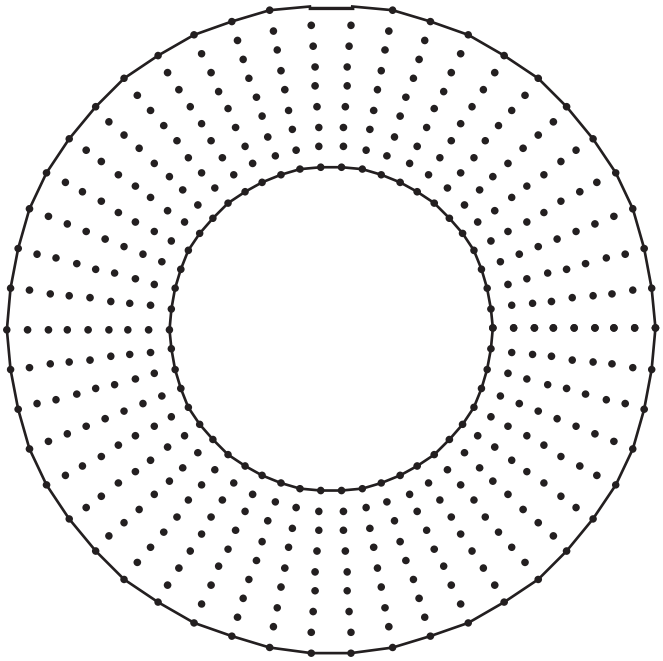

Fig. 6. Nodes arrangement on a torus domain when EFG and IEFG methods are used.

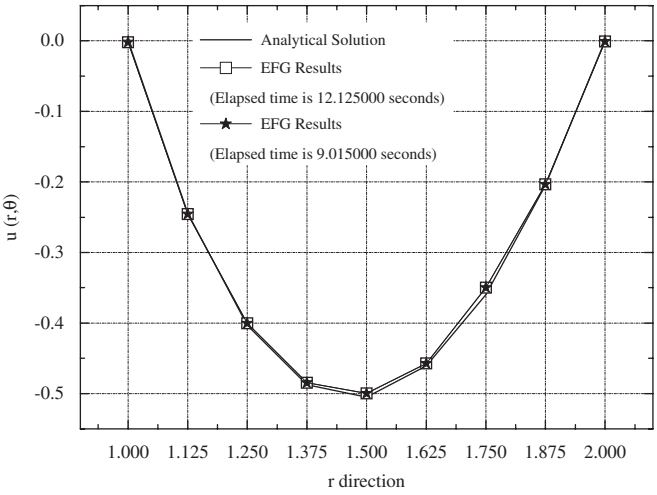

Fig. 7. Results obtained by analytical, EFG and IEFG method along r direction at any angle.

r axis at any angle with $d_{\max}=2.1$ and nodes $=9^{*}51$ are plotted in Fig. 7. In comparison with EFG method, about 25% of the calculation time is saved with IEFG method.

5.2. Laplace equation with mixed boundary conditions on a cube

The next example considered is the 2D Laplace equation with mixed boundary conditions. Supposing a steady temperature field on a rectangular domain, the government equation is

$$\nabla^2 T=\frac{\partial^2 T}{\partial x^2}+\frac{\partial^2 T}{\partial y^2}=0,\quad x\in[0,5],\ \ y\in[0,10], \tag{60}$$

and the boundary conditions are

$$T(x,0)=0,\quad 0<x<5, \tag{61}$$

$$T(0,y)=0,\quad 0<y<10, \tag{62}$$

$$T(x,10)=100\sin(\pi x/10),\quad 0<x<5, \tag{63}$$

and

$$\frac{\partial T(5,y)}{\partial x}=0,\quad 0<y<10. \tag{64}$$

The analytical solution of this temperature field is

$$u(x,y)=\frac{100\sin(\pi x/10)\sinh(\pi y/10)}{\sinh(\pi)}. \tag{65}$$

The regular nodes arrangement when EFG and IEFG methods are used is shown in Fig. 8. Figs. 9 and 10 plot the analytical solution and the numerical solution using the EFG and IEFG methods along the x and y axes, respectively. From the figures, we can see that when $d_{\max}=1.8$ and nodes number is $21^{*}11$; the present results are in total agreement with the analytical solution. Moreover, the computer speed of IEFG is higher than the EFG method.

5.3. Laplace equation with Dirichlet problems on a half-torus domain

As the last example, we consider a 2D Laplace equation with Dirichlet boundary conditions, as shown in Fig. 11. The Laplace's equation is

$$\nabla^2 u=\frac{\partial^2 u}{\partial x^2}+\frac{\partial^2 u}{\partial y^2}=0,\quad r\in[1,2],\ \ \theta\in[0,\pi]. \tag{66}$$

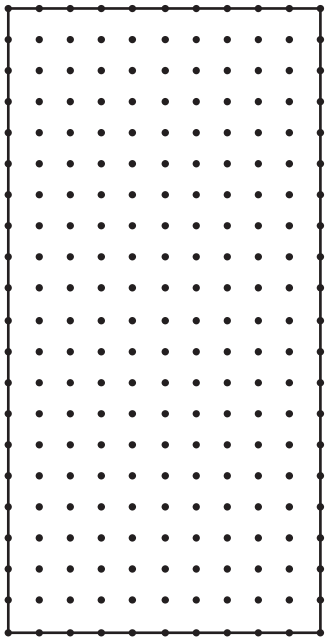

Fig. 8. Regular nodes arrangement on a cubic domain.

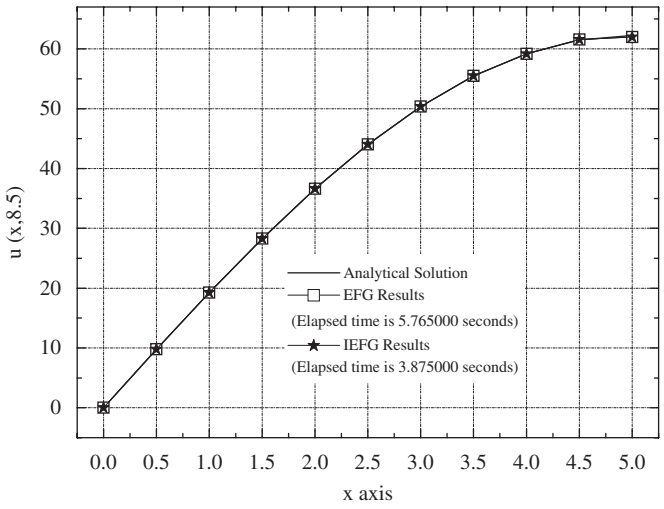

Fig. 9. The temperature distribution along x-axis at $y = 8.5$.

The boundary conditions are

$$u(1,\theta) = \sin(\theta), \quad 0 < \theta < \pi, \tag{67}$$

$$u(2,\theta) = 0, \quad 0 < \theta < \pi, \tag{68}$$

$$u(r,0) = 0, \quad 1 < r < 2, \tag{69}$$

and

$$u(r,\pi) = 0, \quad 1 < r < 2. \tag{70}$$

The analytical solution of this problem is

$$u(r,\theta) = \frac{4}{3} \times \left[\frac{1}{r} - \frac{r}{4}\right] \times \sin(\theta). \tag{71}$$

Figs. 11 and 12 illustrate the comparison between the results calculated using the analytical solution, EFG and IEFG method. It can be seen that when $d_{\max} = 1.2$ and nodes number is 9*51 the methods work well. Compared with the EFG method, the IEFG method has a faster computer time (Fig. 13).

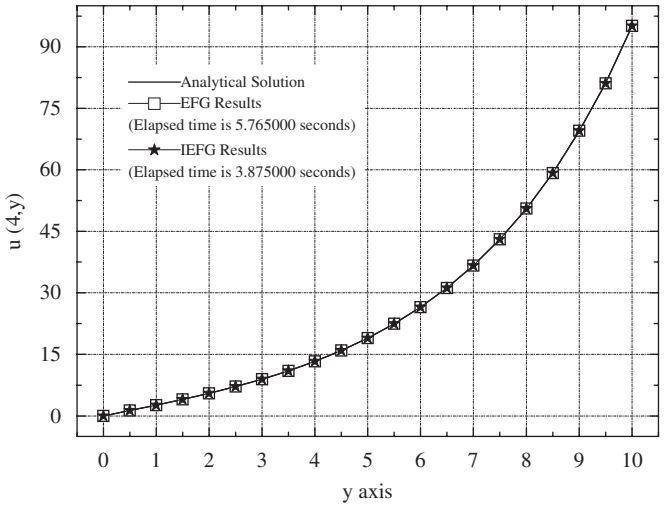

Fig. 10. The temperature distribution along y-axis at $x = 4$.

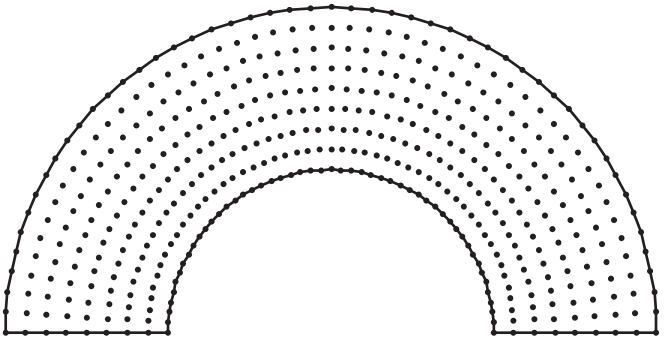

Fig. 11. Nodes planed on a half-torus domain for example 3.

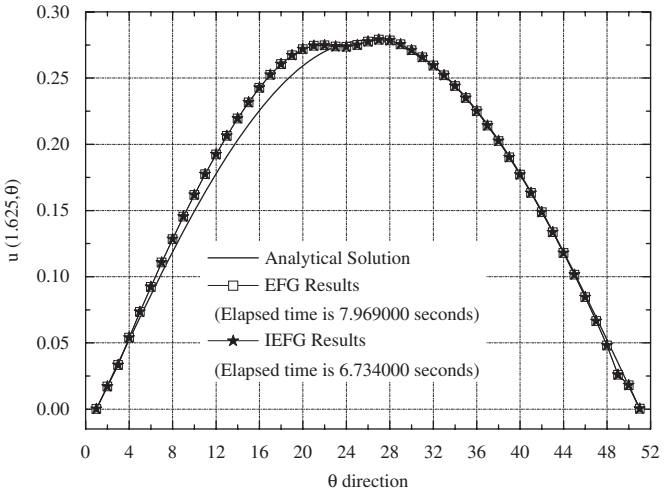

Fig. 12. Compression of the analytical, EFG and IEFG solution along angle axis at $r = 1.625$.

6. Conclusions

This paper proposes an improved element-free Galerkin (IEFG) method that is based on the IMLS for 2D potential problems.

In the IMLS approximation, the orthogonal function system with a weight function is used as the basis function. The IMLS approximation has greater computational efficiency and precision than the MLS approximation, and it does not lead to an

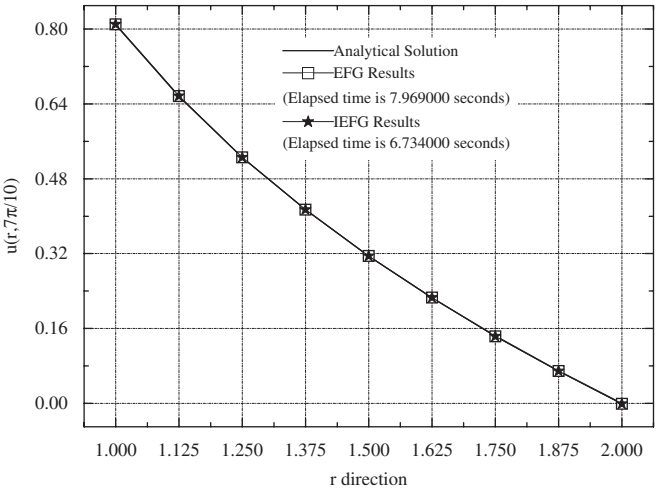

Fig. 13. Values calculated by analytical, EFG and IEFG method along r direction where $\theta = 7\pi/10$.

ill-conditioned system of equations. This means that the system can be solved without obtaining the inverse matrix, and fewer coefficients are involved, thus accelerating the computing speed.

By combining the EFG method and the IMLS approximation method, an improved IEFG method for 2D potential problems is derived. As there are fewer coefficients in the IMLS approximation than in the MLS approximation, and thus in the IEFG method that is formed with the IMLS approximation, fewer nodes are selected in the entire domain than are selected in the conventional EFG method. Hence, the IEFG method should result in a higher computing speed.

Acknowledgement

The work described in this paper was supported by the computing facilities provided by ACIM.

References

[1] Kreyzig Erwin. Advanced engineering mathematics. 8th ed. Wiley; 1999.
[2] Selvadurai APS. Partial differential equations in mechanics 1. Berlin, Heidelberg: Springer; 2000.
[3] Liew KM, Ng TY, Wu YC. Meshfree method for large deformation analysis—a reproducing kernal particle approach. Eng Struct 2002;24:543–51.
[4] Beer G. An efficient numerical method for modeling initiation and propagation of cracks along material interfaces. Int J Numer Meth Eng 1993;36:3579–95.
[5] Belytschko T, Krongauz Y, Organ D, Fleming M, Krysl P. Meshless method: an overview and recent developments. Comput Meth Appl Mech Eng 1996;139:3–47.
[6] Nayroles B, Touzot G, Villon PG. Generalizing the finite element method: diffuse approximation and diffuse elements. Comput Mech 1992;10:307–18.
[7] Belytschko T, Lu YY, Gu L. Element-free Galerkin methods. Int J Numer Meth Eng 1994;37:229–56.
[8] Duarte CA, Oden JT. Hp clouds—a meshless method to solve boundary-value problems. Technical report 95–05. Texas Institute for Computational and Applied Mathematics, University of Texas at Austin, 1995.
[9] Onarte E. A finite point method in computational mechanics. Int J Numer Meth Eng 1996;39:3839–66.
[10] Atluri SN, Zhu TL. A new meshless local Petrov–Galerkin (MLPG) approach in computational mechanics. Comput Mech 1998;22:117–27.
[11] Liu WK, Chen Y, Uras RA, et al. Generalized multiple scale reproducing kernel particle. Comput Meth Appl Mech Eng 1996;139:91–157.
[12] Liu WK, Chen YJ. Wavelet and multiple scale reproducing kernel methods. Int J Numer Meth Fluids 1995;21:901–31.
[13] Chen W. New RBF collocation methods and kernel RBF with applications. In: Griebel M, Schweitzer MA, editors. Meshfree methods for partial differential equations, Vol. 1. Berlin: Springer; 2000.
[14] Idelsohn SR, Onate E, Calvo N, et al. The meshless finite element method. Int J Numer Meth Eng 2003;58:893–912.
[15] Liew KM, Zhao X, Ng TY. The element-free kp-Ritz method for vibration of laminated rotating cylindrical panels. Int J Struct Stability Dyn 2002;2:523–58.
[16] Liew KM, Feng C, Cheng Y, Kitipornchai S. Complex variable moving leastsquares method: a meshless approximation technique. Int J Numer Meth Eng 2007;70:46–70.
[17] Liew KM, Cheng Y, Kitipornchai S. Analyzing the 2D fracture problems via the enriched boundary element-free method. Int J Solids Struct 2007;44:4220–33.
[18] Liew KM, Sun YZ, Kitipornchai S. Boundary element-free method for fracture analysis of 2-D aniotropic piezoelectric solids. Int J Numer Meth Eng 2007;69:729–49.
[19] Liew KM, Cheng Yumin, Kitipornchai S. Boundary element-free method (BEFM) for two-dimensional elastodynamic analysis using Laplace transform. Int J Numer Meth Eng 2005;64(12):1610–27.
[20] Liew KM, Cheng Yumin, Kitipornchai S. Boundary element-free method (BEFM) and its application to two-dimensional elasticity problems. Int J Numer Meth Eng 2006;65(8):1310–32.
[21] Lancaster P, Salkauskas K. Surface generated by moving least squares methods. Math Comput 1981;37:141–58.
[22] Liu GR. Mesh free methods: moving beyond the finite element method. CRC Press LLC; 2003.
[23] Zhang Z, Liew KM, Cheng YM. Coupling of the improved element-free Galerkin and boundary element methods for 2D elasticity problems. Eng Anal Bound Elem 2008;32:100–7.
[24] Zhang Z, Liew KM, Cheng YM, Lee YY. Analyzing 2D fracture problems with the improved element-free Galerkin method. Eng Anal Bound Elem 2008;32:241–50.